

Does the Coralline Alga *Leptophytum foecundum* (Kjellman) Capture Paleoenvironmental Variability in the Arctic Ocean?

Authors: Bougeois, Laurie, Williams, Branwen, Halfar, Jochen, Konar, Brenda, Adey, Walter, et al.

Source: Arctic, Antarctic, and Alpine Research, 47(2) : 375-387

Published By: Institute of Arctic and Alpine Research (INSTAAR),
University of Colorado

URL: <https://doi.org/10.1657/AAAR0014-061>

BioOne Complete (complete.BioOne.org) is a full-text database of 200 subscribed and open-access titles in the biological, ecological, and environmental sciences published by nonprofit societies, associations, museums, institutions, and presses.

Your use of this PDF, the BioOne Complete website, and all posted and associated content indicates your acceptance of BioOne's Terms of Use, available at www.bioone.org/terms-of-use.

Usage of BioOne Complete content is strictly limited to personal, educational, and non - commercial use. Commercial inquiries or rights and permissions requests should be directed to the individual publisher as copyright holder.

BioOne sees sustainable scholarly publishing as an inherently collaborative enterprise connecting authors, nonprofit publishers, academic institutions, research libraries, and research funders in the common goal of maximizing access to critical research.

Does the coralline alga *Leptophytum fœcundum* (Kjellman) capture paleoenvironmental variability in the Arctic Ocean?

Laurie Bougeois^{1,2,3}

Branwen Williams^{1,8}

Jochen Halfar¹

Brenda Konar⁴

Walter Adey⁵

Andreas Kronz⁶ and

Ulrich G. Wortmann⁷

¹Department of Chemical and Physical Sciences, University of Toronto, 3359 Mississauga Road, Mississauga, Ontario L5L 1C6, Canada

²Géosciences Rennes, UMR 6118 CNRS–Université de Rennes 1, 35000 Rennes, France

³Institut des Sciences de la Terre de Paris, UMR 7193 CNRS–Université Pierre et Marie Curie (Paris 6), 75005 Paris, France

⁴Institute of Marine Science, University of Alaska Fairbanks, 217 O'Neill, P.O. Box 757220, Fairbanks, Alaska 99775-7220, U.S.A.

⁵Department of Botany, Smithsonian Institution, P.O. Box 37012, Washington, DC 20013-7012, U.S.A.

⁶Geowissenschaftliches Zentrum der Universität Göttingen, Goldschmidt-Str. 1, D-37077 Göttingen, Germany

⁷Department of Earth Sciences, University of Toronto, 22 Russell Street, Toronto, Ontario M5S 3B1, Canada

⁸Corresponding author. Present address: W. M. Keck Science Department, Claremont McKenna College–Pitzer College–Scripps College, 925 North Mills Avenue, Claremont, California 91711, U.S.A., bwilliams@kecksci.claremont.edu

Abstract

Records of high resolution climate variability in the past are essential to understanding the climate change observed today. This is particularly true for Arctic regions, which are rapidly warming. Prior to instrumental data, proxy records can be extracted from high-latitude climate archives to provide critical records of past Arctic climate variability. Here, we investigate the feasibility of extracting records of climate and environmental variability from the skeleton of the crustose coralline alga *Leptophytum fœcundum* from offshore the Sagavanirktok River in the Beaufort Sea. Although this alga forms an annually banded skeleton, age chronologies were established with difficulty due to the large uncalcified reproductive structures relative to low annual growth rates. Average measurements of skeletal Mg content, $\delta^{18}\text{O}_{\text{alga}}$ values, and $\delta^{13}\text{C}_{\text{alga}}$ values were consistent among the analyzed specimens, but time series of these parameters only significantly correlated between two of the collected specimens for $\delta^{18}\text{O}_{\text{alga}}$. No clear trends in environmental variability explained the patterns in the skeletal geochemistry over time. This suggests that ambient seawater combined with freshwater from the Sagavanirktok River drives the geochemistry of *L. fœcundum* at this site. Thus, coralline algal specimens located near variable sources of low-salinity waters are not ideal organisms to use as proxy archives.

DOI: <http://dx.doi.org/10.1657/AAAR0014-061>

Introduction

The impact of the industrial revolution on climate is a key issue for the global community. To understand recent changes and model future projections of temperature, we need to quantify climate variability during the last several centuries prior to and since the industrial revolution. Because of its importance in modulating climate through changes in albedo, carbon-sink feedbacks, and the Atlantic meridional overturning circulation (AMOC), Arctic paleoenvironments are particularly important for understanding climate variability (ACIA, 2005; Kennett et al., 2003; Kerr, 2010). Approximately 70% of the Arctic Ocean is ice-covered throughout the year, but recent global warming since the mid-19th century has diminished the sea ice extent, changing carbon uptake by the Arctic Ocean (ACIA, 2005; Bauch et al., 2000). The increased fresh-

water flux from both glacial melt and the melting sea ice reduces surface salinity and increases the solubility of CO_2 (Arrigo et al., 2010). As the cold water from the Arctic Ocean contributes to the formation of the North Atlantic Deep Water (NADW), the current freshening of the Arctic Ocean may play a primary role in global climate through slowing the AMOC (Dickson et al., 2007; Jahn and Holland, 2013; Rennermalm et al., 2007). Thus, changes in carbon sink feedbacks and the strength of the AMOC linked to sea-ice melting in the Arctic could influence global climate evolution for the next decades through centuries (ACIA, 2005; Perovich et al., 2007).

Natural proxy archives that give indirect information on past climatic conditions extend environmental data in space and time. At high latitudes, most annual and decadal climate reconstructions are based on terrestrial proxies such as ice cores from glaciers, tree

rings, or varved lake sediments (Kaufman et al., 2009; Overpeck et al., 1997; Steffensen et al., 2008) that do not provide information about marine environmental conditions. The majority of annually to decadal resolved surface ocean climate reconstructions are almost exclusively based on hermatypic shallow-water corals (Grotoli and Eakin, 2007), sclerosponges (Rosenheim et al., 2004), and bivalves (Schöne, 2013). However, hermatypic corals and sclerosponges are limited to tropical and subtropical seas, excluding the possibility of high-latitude climate reconstructions. Although bivalves provide the majority of extratropical near surface marine climate data (e.g., Wanamaker et al., 2011), they also have a limited biogeographical range (Dahlgren et al., 2000). Thus, little is known about the subannual to interannual evolution of the surface Arctic Ocean during the last several centuries, and reconstructions of past climatic variability in the high latitudes would benefit from additional high resolution environmental archives.

The crustose coralline algae *Clathromorphum* sp. and *Lithothamnion glaciale* are ideal biogenic marine climate archives of the mid- to high latitude environmental variability because of their incremental growth pattern, longevity, preservation potential, and incorporation of changes in their ambient environment into the geochemistry and sclerochronology of their skeleton (Chan et al., 2011; Halfar et al., 2013, 2008; Hetzinger et al., 2013; Kamenos et al., 2008, 2012; Williams et al., 2011). Seasonal decreases in temperature and light during winter periods reduce the calcification rate of the algae. The skeletal anatomy changes from narrow and elongate cells with dense walls to wider and shorter cells with thinner walls resulting in growth increment demarcations in the fall to early winter in its high Mg-calcite skeleton (Adey et al., 2013). Furthermore, cavities in which the reproductive structures develop (i.e., sporangial conceptacles) form in fall and early winter (Adey, 1966) in *Clathromorphum* sp. Parts of the conceptacles intrude downward by decalcification, protruding into algal skeleton that has precipitated in the summer. Nevertheless, yearly layering of conceptacle cavities can provide a secondary marker for annual growth (Adey, 1966). Diagenesis resulting from the decalcification is limited to the skeleton within 1–2 microns of the conceptacles. In cases of minimal yearly growth, conceptacle bases can intrude into the previous year's growth (Moberly, 1968). Yet, to date, reconstructions derived from *Clathromorphum* sp. and *L. glaciale* in the Arctic Ocean are limited (Halfar et al., 2013; Kamenos, 2011) due to a lack of sufficient higher latitude specimens. Thus, additional studies are needed to increase the use of coralline algae to reconstruct Arctic climate change.

The high-latitude crustose coralline alga *Leptophytum fæcundum* (Kjellman) may serve as a paleoenvironmental proxy to increase the number and spatial extent of records of environmental change in the Arctic Ocean. Thus, we measured growth rates and growth increment formation along with Mg/Ca, $\delta^{18}\text{O}$, and $\delta^{13}\text{C}$ composition of the high-Mg calcitic skeleton in three specimens from the Beaufort Sea to evaluate the feasibility of extracting environmental signals from the skeleton of *L. fæcundum*. If this alga proves to yield a reliable record of Arctic Ocean parameters, future studies may use longer-lived specimens in order to reconstruct the climate evolution of the Arctic Ocean during the past centuries during which we have no instrumental data.

Methods

STUDY AREA

Three specimens of the coralline alga *Leptophytum fæcundum* (Kjellman) (BSA2, BSA3, and BSA7) were collected live from 5 m depth by SCUBA during a research cruise in the

Beaufort Sea, close to Prudhoe Bay, off the Sagavanirktok River (Sag River) delta (70°20'N, 147°40'W) in July 2007 (Fig. 1). Sea surface temperatures (SSTs) derived from OBPQ Aqua MODIS Ocean Color for the sampling site vary from $-1.95\text{ }^{\circ}\text{C}$ in the winter season (December through April/May) to $5\text{ }^{\circ}\text{C}$ in July over the period of 2002–2008 (Acker and Leptoukh, 2007). On shore, the 289 km Sag River originates on the north slope of the Brooks Range in northern Alaska (Benke and Cushing, 2011) then flows across the Arctic Slope province before entering the Beaufort Sea in the Arctic Ocean (Fig. 1). It is principally fed by snowmelt with some groundwater and glacial influence (Benke and Cushing, 2011) and is frozen between September and May, thawing in late May to June. Surface temperatures for the Sag River have varied from $0\text{ }^{\circ}\text{C}$ to $15\text{ }^{\circ}\text{C}$ between 1990 and 2007 (temperatures provided by Mathew Schellekens [USGS]). Annual Sag River discharge and gage height vary from 28 to $69\text{ m}^3\text{ s}^{-1}$ and 5 to 7 m, respectively, on interannual time scales (Fig. 2, parts a and d) (data from <http://waterdata.usgs.gov>).

Leptophytum fæcundum (KJELLMAN)

Leptophytum fæcundum is an Arctic species that extends into the subarctic photic zone (Adey, 1970) and grows on pebbles and stones (Athanasiadis and Adey, 2006) (Fig. 3). It is a crustose species with no major surface irregularity, except those created by overgrowing over an irregular substrate (Athanasiadis and Adey, 2006). Overgrowth of one plant by another is rare in this species (Adey et al., 2001). Buried multiporate asexual conceptacles ranging from 220 to 500 μm in diameter and 140 to 250 μm in height are very frequent (*L. fæcundum* var. *sandrae*) (Athanasiadis and Adey, 2006). Lateral growth rates based on specimens grown in laboratory experiments range from 1 to $9\text{ }\mu\text{m day}^{-1}$ ($= 365$ to $3285\text{ }\mu\text{m yr}^{-1}$), depending on ambient temperature and light (Adey, 1970).

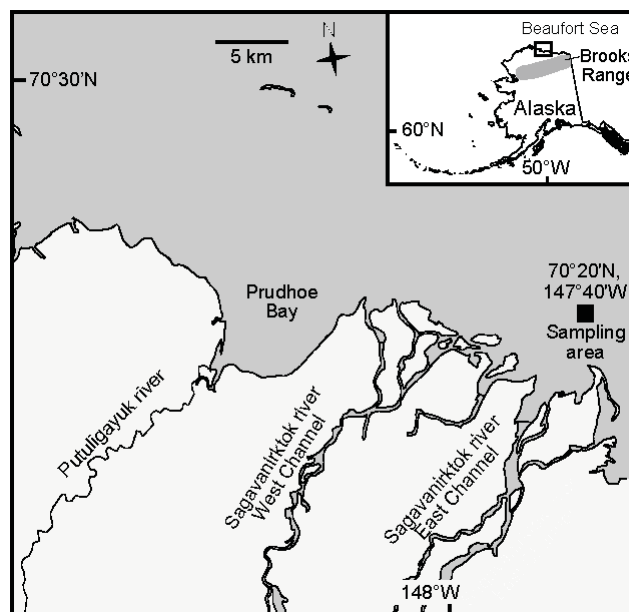


FIGURE 1. Study area in Beaufort Sea showing proximity to Prudhoe Bay and Sagavanirktok River, including the Sag River delta (inspired from Kline et al., 1998).

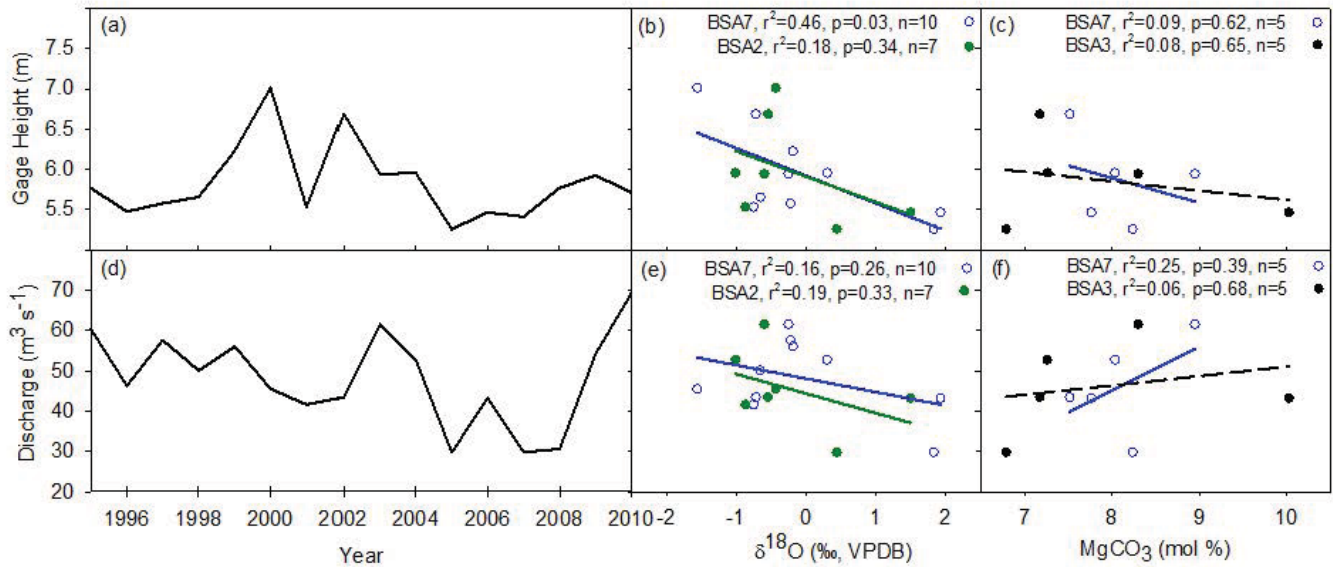


FIGURE 2. (a) Gage height with time; (b) gage height versus $\delta^{18}\text{O}$ composition and (c) MgCO_3 content. (D) Discharge data for Sagavanirktok River (data from <http://waterdata.usgs.gov>) with time, (e) discharge data versus $\delta^{18}\text{O}$ composition, and (f) MgCO_3 content.

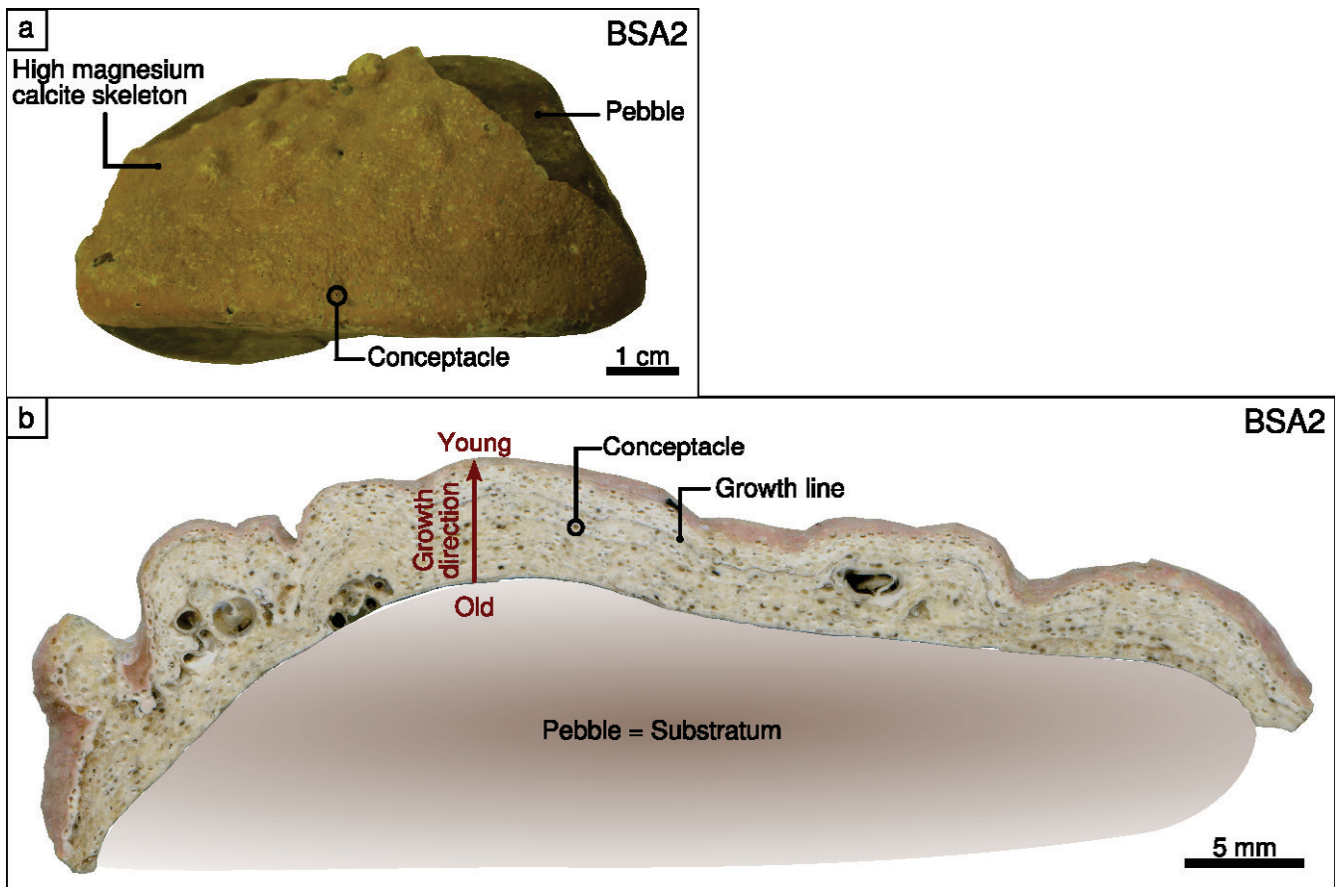


FIGURE 3. Anatomical characteristics of *L. fæcundum* calcareous skeleton. (a) *L. fæcundum* in life position growing on pebble (top view). (b) Cross section of *L. fæcundum* (BSA2) perpendicular to growth direction showing growth direction, growth lines, and conceptacles.

SAMPLE PREPARATION AND ANALYSIS

After collection, a dozen of *L. fecundum* specimens were air dried, separated from pebbles, and cut into 1-cm-thick slices perpendicular to the direction of growth using a circular diamond precision saw (Buehler IsoMet1000). Three specimens with the highest potential to record paleoenvironmental data based on largest vertical height and best developed growth lines were selected for further visual and geochemical analyses. These samples were epoxyed onto glass slides and machine polished to 1 μm with a Logitech CL50 using diamond-polishing suspensions with grit sizes of 9, 3, and 1 μm on a Buehler polishing disk. Polished sections were cleaned in an ultrasonic bath for 10 minutes with deionized water between each polishing step and dried overnight prior to sampling.

Digital images of the polished surface were produced using an Olympus reflected light microscope (VS-BX) attached to an automated sampling stage-imaging system equipped with geo.TS software (Olympus Soft Imaging Systems). This setup allows a two-dimensional mapping of the surfaces of the polished specimens using multiple images spliced together to generate one image. The resulting high resolution photomosaics enabled the identification of growth patterns over the entire sample and the subsequent selection of sampling locations (Fig. 4). The locations of conceptacles and annual growth increments were identified using the digital photomosaics.

Mg/Ca MEASUREMENTS

Mg/Ca values in specimens BSA3 and BSA7 were measured using a JEOL JXA 8900 RL electron microprobe at the University of Göttingen, Germany. For quantitative wavelength dispersive measurements, an acceleration voltage of 15 kV, a focused beam, and a beam current of 12 nA were used (see Hetzinger et al., 2009, for additional details). The electron beam was manually positioned on calcite within an individual algal cell. The sampling transects were preselected on the digital photomosaic images avoiding conceptacle cavities and recalcified portions of the skeleton (Fig. 4). Spot analyses were spaced 10 μm apart along a transect parallel to the direction of growth (Figs 4 and 5). Transects ranged in length from 890 μm (BSA3) to 1440 μm (BSA7). Counting statistics errors at the 99% confidence level varied between 0.035 and 0.087 mass % for MgO and between 0.33 and 0.40 mass % for CaO. The detection limit of MgO calculated from the background noise was 100 $\mu\text{g g}^{-1}$ at the 99% confidence level. Backscattered electron images obtained after the microprobe analysis documented the actual single point transects analyzed (Appendix Fig. A1).

The substitution of Ca by Mg in calcium carbonate is an endothermic reaction, thus it is favored by higher temperatures, providing the use of Mg/Ca ratio as a paleothermometer (Lear, 2002). Seasonally changing Mg content within annually banded coralline algae positively correlates to the sea surface temperatures (SSTs) of the water in which they formed (Chave, 1954; Adey, 1965; Chave and Wheeler Jr., 1965; Hetzinger et al., 2009; Kamenos et al., 2008), although light- and temperature-driven growth rates may also influence Mg content (Kolesar, 1978; Moberly, 1968). Using the *Lithothamnion glaciale* MgCO₃-SST relationship established by Halfar et al. (2000) the mol% values measured here were converted to temperature:

$$T(^{\circ}\text{C}) = 0.97 \times \text{MgCO}_3(\text{mol}\%) - 7.90. \quad (1)$$

In addition, the MgO and CaO values measured here were translated into Mg/Ca values (mol/mol) and then converted to temperature using the *Clathromorphum nereostratum* Mg/Ca-SST relationship established by Williams et al. (2014) for a different genus of coralline algae:

$$T(^{\circ}\text{C}) = 87.53 \times \text{Mg/Ca} (\text{mol/mol}) - 5.46. \quad (2)$$

DEVELOPMENT OF CHRONOLOGY

Chronologies were generated first by counting annual growth lines on the mapped and digitized image of the specimens. All samples were live collected; hence the top layer was assigned the year of collection, 2007, and calendar years were assigned to annual growth increments starting from 2007 and extending back in time. In addition, yearly growth-increment widths were calculated from annual Mg/Ca-element cycle widths that were obtained by electron microprobe for two specimens (BSA3 and BSA7). Age models were established on the basis of the seasonal cycle in algal Mg/Ca: high Mg values within the skeleton were assigned to July, which is on average the warmest month, and minimum values were tied to February, which is on average the coolest month at the study site (Benke and Cushing, 2011). The algal Mg/Ca time series were linearly interpolated between these anchor points using the AnalySeries software (Paillard et al., 1996) to obtain an equidistant proxy time series with a monthly resolution. Because of possible growth discontinuities prior to the year 2001 in BSA3 and 1997 in BSA7, only data after those years were interpreted. Linear regression tested for statistical correlation of the monthly resolved time-series between the two specimens, and with instrumental records of environmental conditions. The developed chronologies were refined and cross-checked for possible errors in the age model by comparing annual extreme values in the Mg/Ca ratio time series to mapped growth increment patterns for each individual year of algal growth.

STABLE OXYGEN AND CARBON ISOTOPE ANALYSIS

Skeletal material for stable oxygen and carbon isotopes analyses was removed in specimens BSA2 and BSA7 by a high-precision, computer-driven New Wave Research Micromill attached to an x, y, and z stage using digitized milling path positions. Due to logistical constraints, we did not determine the isotopic composition of specimen BSA3. For specimens BSA2 and BSA7, sampling paths were defined using geo.TS software and transferred to the Micromill to mill 100 to 200 μg of calcite powder per sample resulting in a resolution of two to four samples per year. The sampling depth was 150 μm and sample path lengths averaged 1.30 cm for BSA2 and 1.15 cm for BSA7. Since skeletal material was bulk sampled to obtain sufficient material for analysis, conceptacles were not avoided. Material was removed from the outside edge of the specimen first, which represented the most recent growth followed by subsequent samples moving toward the oldest part of the sample. Using a razor blade, the milled powder was transferred into a glass vial used for the mass spectrometer. Sample amounts were 56 samples milled from BSA2 and 42 from BSA7.

Removed material was analyzed for $\delta^{18}\text{O}$ and $\delta^{13}\text{C}$ (‰ relative to Vienna Pee Dee Belemnite standard [VPDB]) using a Thermo-Finnigan MAT253 mass spectrometer connected to a gasbench and autosampler at the Geobiology Stable Isotope Lab-

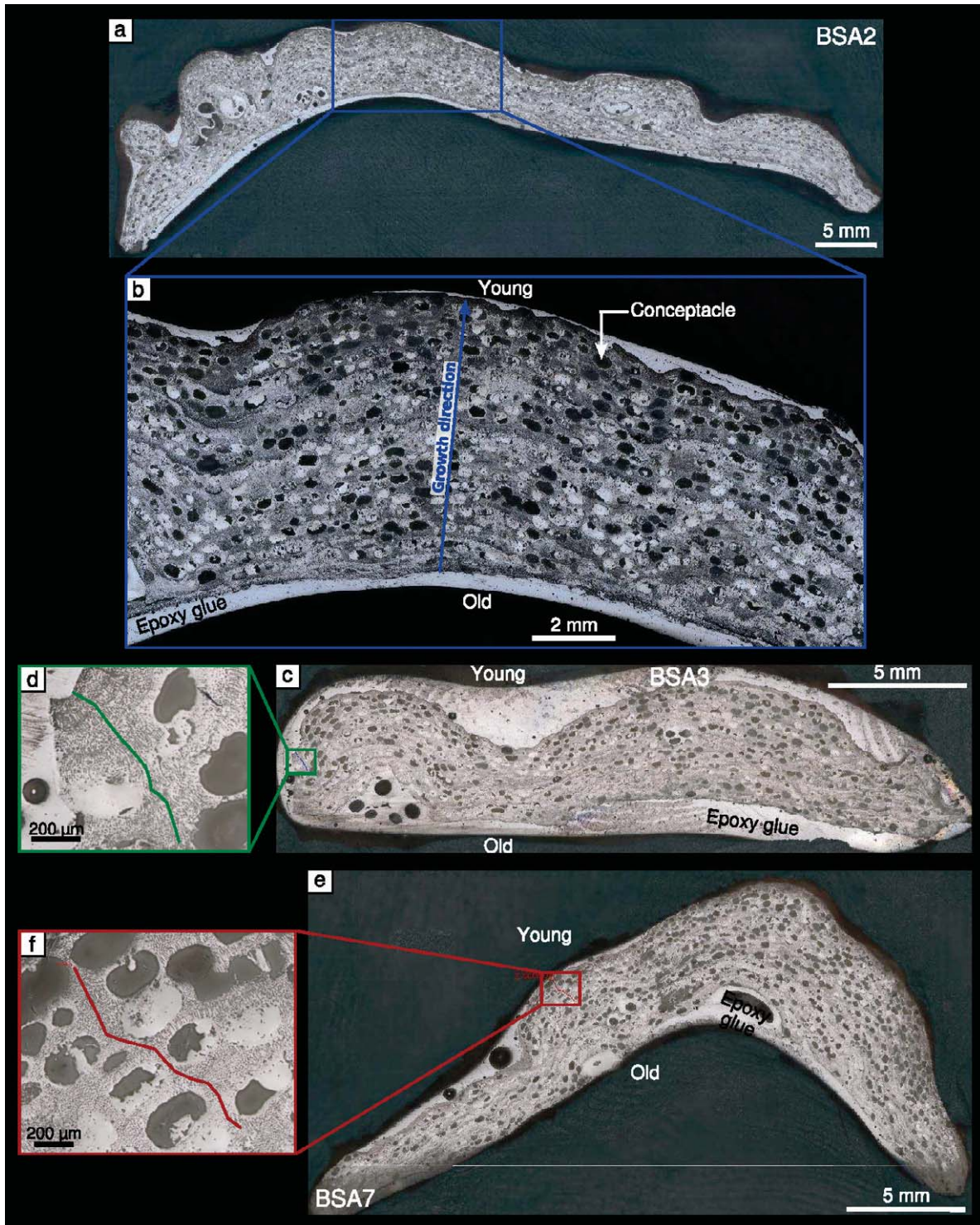


FIGURE 4. Geo.TS images of (a and b) BSA2, (c) BSA7, and (e) BSA3 cross sections with selected transects for microprobe measurements for (d) BSA3 and (f) BSA7.

oratory, University of Toronto. The international standard NBS-19 and two in-house standards (IAEA-CO-1 and IAEA-CO-2) were used for calibration of all samples. One standard deviation of the mean of duplicate measurements was $\pm 0.08\text{‰}$ for $\delta^{18}\text{O}$ and $\pm 0.16\text{‰}$ for $\delta^{13}\text{C}$. Using the established chronology, a stable isotope time series was compiled for BSA2 and BSA7.

Since stable oxygen isotope fractionation during calcification is temperature dependent, the $\delta^{18}\text{O}$ composition of calcium carbonates serves as a paleothermometer (Urey, 1947). Here, seawater temperatures were reconstructed using the temperature-oxygen isotope calibration established by Anderson and Arthur (1983) with modifications to account for the high Mg

content (Jiménez-López et al., 2004) and vital effects (Halfar et al., 2008):

$$T(^{\circ}\text{C}) = 16 - 4.14 \times (\delta^{18}\text{O}_{\text{c}} - \delta^{18}\text{O}_{\text{sw}} + 3.5) + 0.13 \times (\delta^{18}\text{O}_{\text{c}} - \delta^{18}\text{O}_{\text{sw}} + 3.5)^2 + 0.17 \times \text{mol\% MgCO}_3. \quad (3)$$

A $\delta^{18}\text{O}_{\text{sw}}$ value of -4.49‰ (Bedard et al., 1981; Schmidt et al., 1999) was used, which is consistent with end-member seawater values reported by Alkire and Trefry (2006) for seawater $\delta^{18}\text{O}$ composition.

Results

CHRONOLOGY

The combination of a high number of large conceptacles and very low growth rates resulted in poorly delimited annual growth increments (Figs. 4 and 5). Despite this, image-based chronologies were established from 1997 to 2007 for BSA7, from 2000 to 2007 for BSA2, and 1998 to 2007 for BSA3. Average annual growth rates were $180 \pm 26 \mu\text{m yr}^{-1}$ (max = $213 \mu\text{m yr}^{-1}$, min = $117 \mu\text{m yr}^{-1}$) for BSA2, $243 \pm 49 \mu\text{m yr}^{-1}$ (max = $330 \mu\text{m yr}^{-1}$, min = $160 \mu\text{m yr}^{-1}$) for BSA7, and $190 \pm 50 \mu\text{m yr}^{-1}$ (max = $243 \mu\text{m yr}^{-1}$, min = $109 \mu\text{m yr}^{-1}$) for BSA3 (Table 1) (Fig. 6, part a).

Maxima in Mg/Ca were aligned with the center of each growth increment, and minima with growth increment lines in BSA3 and BSA7 resulting in ~ 15 samples year $^{-1}$ for BSA3 and ~ 21 samples year $^{-1}$ for BSA7 prior to interpolation. Using widths of the annual Mg/Ca cycle, annual growth rates averaged $215 \pm 50 \mu\text{m}$ from 2001 to 2006 for BSA7 and $170 \pm 47 \mu\text{m}$ from 2003 to 2006 for BSA3 (Table 1). The Mg/Ca-derived growth rates were comparable to the growth rates measured using the visual growth increments as a reference.

Mg CONTENT

The average MgCO_3 content did not significantly differ between the specimens BSA3 and BSA7 ($p = 0.36$, $n = 57$; Table 1). Using monthly interpolated values, the MgCO_3 content did not significantly correlate between the two specimens ($p = 0.82$, $r^2 = 0.03$, $n = 57$; Fig. 6, part b).

Using Equation 1, reconstructed temperatures averaged $-0.05 \pm 2.0^{\circ}\text{C}$ (min = -3.9°C , max = 3.9°C) for BSA3 (period: 2001–2006) and $-0.3 \pm 1.9^{\circ}\text{C}$ (min = -4.5°C , max = 4.5°C) for BSA7 (period: 2000–2006; Fig. 7, parts b and c). Using Equation 2, reconstructed temperatures averaged $2.3 \pm 2.1^{\circ}\text{C}$ (min = -1.7°C , max = 6.6°C) and $2.1 \pm 2.0^{\circ}\text{C}$ (min = -2.4°C , max = 7.2°C) for BSA3 and BSA7, respectively, for the same periods as above (Fig. 7, parts b and c). Using annually averaged values, neither temperature reconstruction significantly correlated with satellite-derived SST ($p = 0.37$, $r^2 = 0.12$, $n = 57$ and $p = 0.55$, $r^2 = 0.07$, $n = 72$ for BSA3 and BSA7, respectively).

STABLE OXYGEN ISOTOPE VALUES

The $\delta^{18}\text{O}_{\text{alga}}$ values did not significantly differ between the specimens BSA2 and BSA7 ($p = 0.30$, $n = 7$; Table 1). Using annually averaged values, the $\delta^{18}\text{O}_{\text{alga}}$ values significantly correlated between the two specimens from 2000 to 2006 ($p = 0.045$, $r^2 = 0.59$, $n = 7$; Fig. 6, part c). Neither of the annually averaged $\delta^{18}\text{O}_{\text{alga}}$ records significantly correlated with growth rates or Sag River discharge or streamflow. The $\delta^{18}\text{O}_{\text{alga}}$ record for specimen BSA7 significantly

correlated with gage height from 1997 to 2006 ($p = 0.03$, $r^2 = 0.46$, $n = 10$; Fig. 2, part b).

Using Equation 3, the oxygen isotopic composition of *L. foecundum* yielded average seawater temperatures of $-0.22 \pm 0.99^{\circ}\text{C}$ and $-0.03 \pm 1.12^{\circ}\text{C}$ for specimens BSA2 and BSA7, respectively (Fig. 7, parts d and e). Neither temperature reconstruction significantly correlated with satellite-derived SST ($p = 0.74$, $r^2 = 0.16$, $n = 7$ and $p = 0.76$, $r^2 = 0.11$, $n = 10$ for BSA2 and BSA7, respectively).

STABLE CARBON ISOTOPE VALUES

The average (\pm stdev) $\delta^{13}\text{C}_{\text{alga}}$ values significantly differed between the specimens BSA2 and BSA7 ($-1.93\text{‰} \pm 0.18\text{‰}$ and $-1.59\text{‰} \pm 0.31\text{‰}$, respectively) for the common period 2000–2006 ($p = 0.0009$, $n = 14$) (Fig. 6, part d). Using annually averaged values, the $\delta^{13}\text{C}_{\text{alga}}$ values did not significantly correlate between the two specimens, or with Sag River discharge or gage height. The annually averaged $\delta^{13}\text{C}_{\text{alga}}$ values significantly correlated with annual growth rates in specimens BSA2 ($p = 0.014$, $r^2 = 0.86$, $n = 7$) but not BSA7.

Discussion

DEVELOPMENT OF CHRONOLOGY

The large conceptacles (140–250 μm diameter) relative to very low growth rates (180 to 240 $\mu\text{m yr}^{-1}$) obscured the annual growth bands in some instances. In addition, not all growth increments identified in the digital images of each specimen were continuous laterally, and growth interruptions distorted the chronology because their duration was unknown (Fig. 5). Thus, chronologies prior to growth discontinuities in each specimen were not assigned (Table 1). Despite this, measured growth rates in the specimens were similar to thickness growth rates obtained for Arctic to Subarctic species of the climate archive *Clathromorphum compactum* (Adey et al., 2013). Cross dating of both algae using the same method as for tree rings (i.e., to correlate years with the same thickness of growth increments) was not possible because a variety of specimen-specific biotic factors alters growth, including shading of a specimen for an extended period, differential grazing, and/or other unknown factors. The chronology deduced from the width of annual Mg/Ca cycles was established with difficulty because of noise in the elemental signal (Fig. 6, part b), likely resulting from the small-scale variability in annual growth banding and the sometimes low seasonal variability in seawater surface temperatures (Fig. 7, part a). Despite this, growth rates determined from the annual cycle in Mg content were consistent with those determined from the optically measured growth increment widths. The difficulty in determining the growth increments and short lifespans in the specimens collected, along with restricted development of the perithallium (Adey et al., 2001), indicates that long-lived specimens of this species with clear chronologies may be difficult to find. Newer collections of this species from the Labrador Sea Coast, unaffected by freshwater influent appear more regular and may provide better climate archive data (Adey, specimens in herbarium US).

Mg/Ca-DERIVED SEA SURFACE TEMPERATURES

SSTs reconstructed using the *L. glaciale*-derived transfer function yielded similar average temperatures to the satellite SST data ($\leq 0.7^{\circ}\text{C}$ difference, Fig. 7, parts a and b); however, the winter minima far exceeded satellite values (e.g., $-3.9^{\circ}\text{C}_{\text{alga}}$ and $-4.5^{\circ}\text{C}_{\text{alga}}$ vs. $-1.8^{\circ}\text{C}_{\text{satellite}}$). SSTs reconstructed using the *C. nereostratum*-derived transfer function yielded average reconstructed SSTs exceeding the

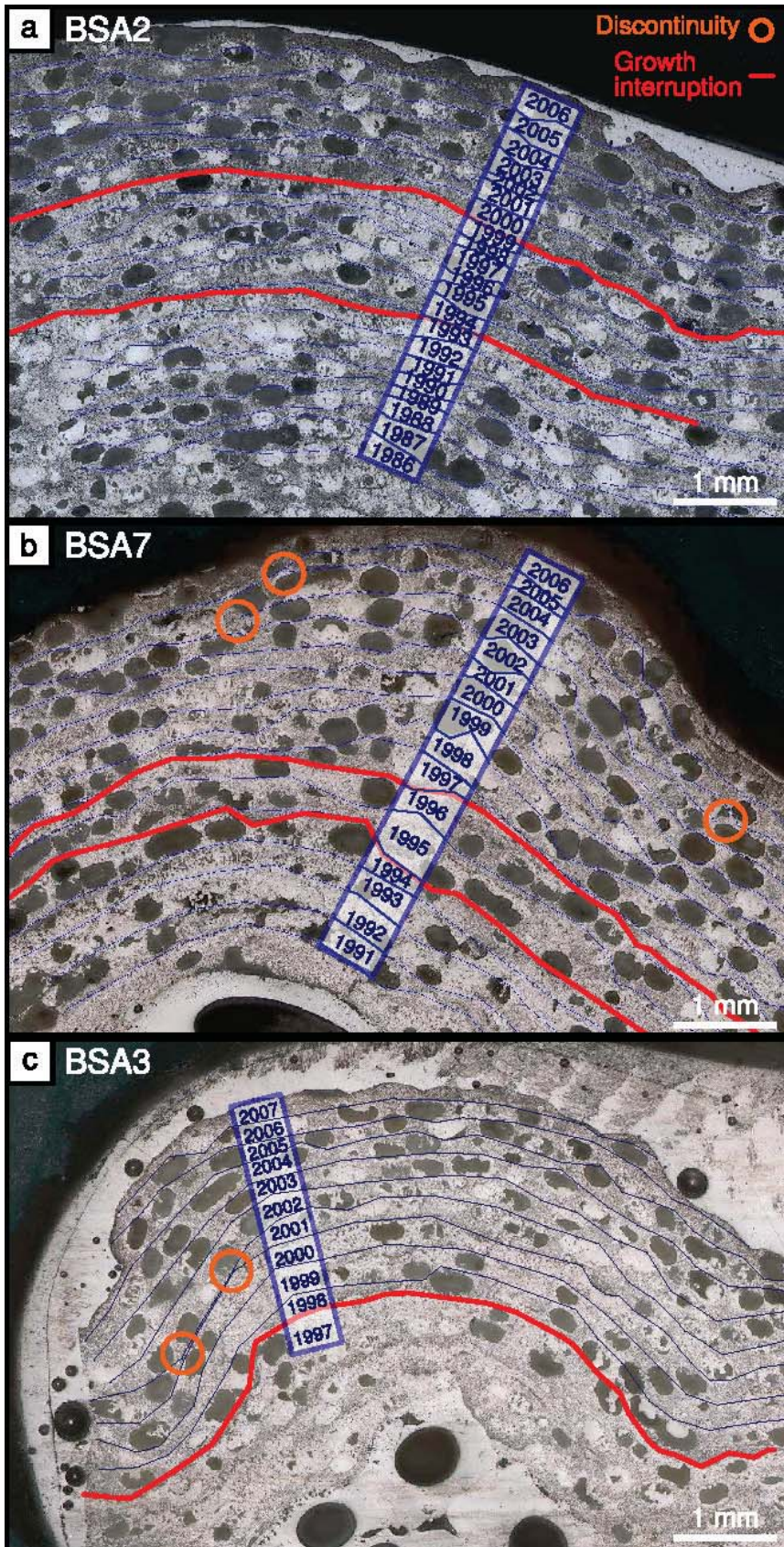


FIGURE 5. Chronologies for (a) BSA2, (b) BSA7, and (c) BSA3. Blue lines delimit annual growth increments. Calendar years were assigned to annual growth increments starting from the year of collection and extending back in time. Red lines underline a growth interruption across an entire year, and orange circles point to discontinuities where a section of growth is missing within a single year.

satellite SST data (2.8–3.0 °C difference) due to overestimation of the summer maxima (e.g., 6.6 °C_{alga} and 7.2 °C_{alga} vs. 2.8 °C_{satellite}) (Fig. 7, parts a and b). Thus, the transfer functions developed for

other coralline algal species cannot be applied successfully to *L. fecundum*, potentially due to taxa-specific vital effects or because of site-specific environmental variability. Such differences between

TABLE 1

Calculated average growth rates, MgCO₃ (Mol%), and δ¹⁸O and δ¹³C (‰, VPDB) values for each specimen. Mg/Ca was not measured in BSA2 and stable isotopes were not measured in BSA3.

Specimen	Growth increments	MgCO ₃ (Mol%) measurements	δ ¹⁸ O and δ ¹³ C measurements
BSA2	Growth rates: 183 ± 30 μm yr ⁻¹ (2000–2006)		δ ¹³ C: -1.95 ± 0.15 (2000–2006) δ ¹⁸ O: -0.75 ± 0.22 (2000–2006)
BSA3	Growth rates: 178 ± 26 μm yr ⁻¹ (2001–2006)	Growth rates: 170 ± 47 μm yr ⁻¹ (2001 to 2006) MgCO ₃ (Mol%): 8.06 ± 2.04 (2001–2006)	
BSA7	Growth rates: 214 ± 35 μm yr ⁻¹ (1997–2006)	Growth rates: 215 ± 50 μm yr ⁻¹ (2000–2006) MgCO ₃ (Mol%): 7.81 ± 1.91 (2000–2006)	δ ¹³ C: -1.69 ± 0.33 (1998–2006) δ ¹⁸ O: -0.80 ± 0.28 (1998–2006)

SST and bottom temperature necessitate *in situ* calibrations for coralline algae or just a species-specific calibration. In addition, it is apparent from parallel studies of the high latitude climate archive *C. compactum* that growth can cease for a number of months in mid-winter, during the later phases of Arctic winter darkness, further complicating coralline archives from different latitudes.

Salinity affects the incorporation of Mg into the skeleton of the alga *C. nereostratum* (Chan et al., 2011), hence a freshwater influence from the Sag River may alter the incorporation of Mg in the skeleton to changes in temperature. Recent studies of high-Mg calcite in echinoderm skeletons and foraminiferal tests field-collected or cultured in different salinities have demonstrated a clear negative effect of salinity on Mg/Ca ratios (Ferguson et al., 2008; Kısakürek et al., 2008). This effect might explain the cold temperatures calculated in this study using the *L. glaciale*-derived transfer function, as the salinity in Beaufort Sea is very low (between 15‰ and 30‰) and the Sag River contributes significant amounts of freshwater to the collection site. More experiments that monitor temperature and salinity would therefore be necessary to establish a new calibration linking MgCaO (mol%) and temperature in waters with low salinity. Regardless, our data indicate that without further exploration, *L. fecundum* cannot be used as a paleo-SST proxy in the Arctic Ocean using skeletal Mg content.

OXYGEN ISOTOPE VALUES

SSTs reconstructed from the algal-δ¹⁸O composition generated average seawater temperatures that were consistent with the satellite SST data (Fig. 7, parts a and d). Thus, seawater temperature is a primary control driving the δ¹⁸O composition of *L. fecundum* at this location. However, the algal-derived SSTs do not significantly correlate with the satellite SSTs at interannual timescales, nor do they vary seasonally as is evident in the satellite data. Thus, other factors in addition to seawater temperature drive the temporal variability in skeletal oxygen isotopic composition. Given that the oxygen isotopic record does not vary consistently subannually, seasonal freezing and melting of sea ice with isotopically light δ¹⁸O likely does not influence the oxygen composition of the algal skeleton. Indeed, even if seawater becomes enriched in ¹⁸O as it freezes, the isotopic fractionation observed in sea ice is typically small (Cooper et al., 2005). Instead, runoff from Sag River likely influences the isotopic composition off the delta, along with other factors. As the source of Sag River is located in the high altitudes of the Brooks Range in Alaska with a continental climate, the runoff is strongly depleted in ¹⁸O (Cooper et al., 2005). In addition, Sag River temperatures are significantly warmer than the Beaufort Sea (Fig. 7, part a). As such, enhanced Sag River runoff would be expected to drive nega-

tive deviations in the alga δ¹⁸O composition, which is not supported by the data here. Thus, while the δ¹⁸O_{alga} variations of the two specimens significantly correlate with each other, supporting a common environmental driver of alga δ¹⁸O composition and suggesting that specimen-specific variables such as diagenesis of the conceptacles is not a concern, seawater temperature and salinity, and fresh water from the Sag River likely combine to influence the oxygen isotopic composition. In addition, *L. fecundum* may integrate the ambient water δ¹⁸O signal over several years, further compounding the drivers of the alga's oxygen isotopic composition.

CARBON ISOTOPE VALUES

Intrinsic characteristics of each specimen may control the δ¹³C_{alga} composition. Generally, more negative δ¹³C_{alga} values are associated with faster rates of skeleton formation in other calcium carbonate marine organisms (Butler et al., 2011; Swart et al., 2010). In fact, the δ¹³C_{alga} may reflect kinetic isotopic disequilibrium at high growth rates. During the years of relatively low growth rates, a relative increase in the proportion of metabolic carbon available for skeleton construction may deplete the skeletal ¹³C (Butler et al., 2011; Lorrain et al., 2004). Thus, an increase in extension rate is coupled with a decrease in δ¹³C_{alga} and vice versa. However, growth rates positively correlate with δ¹³C_{alga} in specimen BSA2, while no clear pattern is present in specimen BSA7 (Fig. 6, part d). Therefore, the source of variability in the skeletal δ¹³C_{alga} values may not in fact be intrinsic to the coralline alga. Exploration of external factors driving δ¹³C_{alga}, changes in the ambient dissolved inorganic carbon (DIC) that is the source of carbon to the algae, may thus be useful.

Anthropogenic burning of isotopically light fossil fuels is decreasing the isotopic composition of the carbon in the atmosphere and the oceans. This century-scale trend toward lighter carbon isotopes—the δ¹³C-Suess effect (Nozaki et al., 1978; Suess, 1953)—is recorded in calcareous skeletons of long-lived marine organisms (Swart et al., 2010). A decline in δ¹³C of -0.95‰ per decade for the 1990s was measured in coralline algae in the northern North Pacific Ocean/Bering Sea (Williams et al., 2011), and -0.9‰ from 1850 to 1987 in the Arctic Ocean in the polar planktic foraminifer *Neogloboquadrina pachyderma* (Bauch et al., 2000). These rates are high relative to values measured in other areas of the world oceans in low latitudes and may represent changes in ventilation of the surface waters (Bauch et al., 2000; Williams et al., 2011). Here, the clear absence of a decreasing trend for δ¹³C_{alga} in BSA2 and BSA7 implies that anthropogenic carbon is either not being taken up by the ocean locally or the decreasing isotopic composition of the DIC is being offset by other processes. The Beaufort Sea is partly sea-ice covered all year round (Pabi et al.,

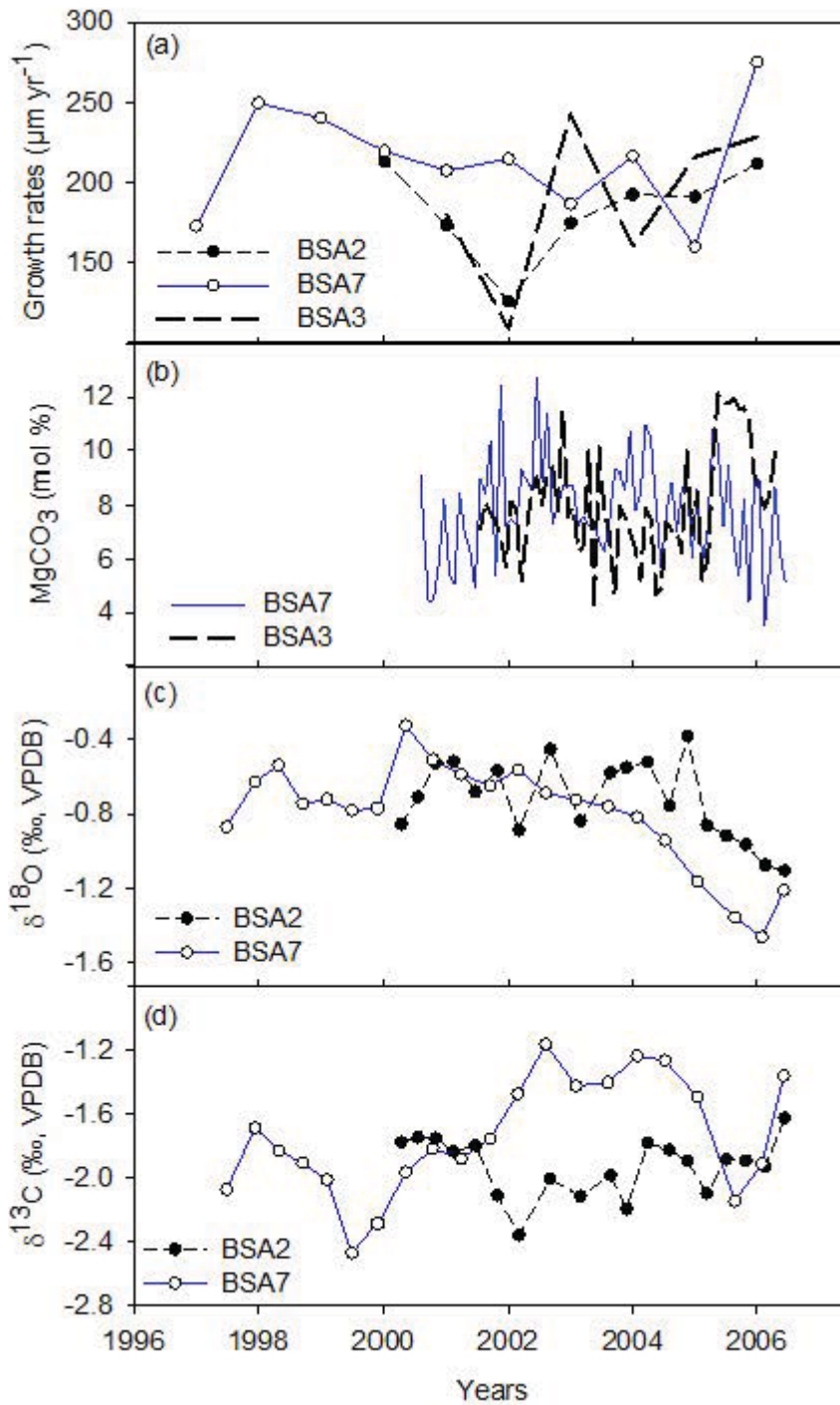


FIGURE 6. Measured (a) growth rates ($\mu\text{m yr}^{-1}$), (b) MgCO_3 (mol%), (c) $\delta^{18}\text{O}$ (‰, VPDB), and (d) $\delta^{13}\text{C}$ (‰, VPDB) for each specimen analyzed.

2008), which could decrease the exchange between atmosphere and ocean and can explain the absence of an oceanic Suess effect in the Beaufort Sea. Alternatively, a potential increase in primary productivity in the Beaufort Sea (Pickart et al., 2013; Tremblay et al., 2011) may be offsetting the decline in skeletal $\delta^{13}\text{C}_{\text{alga}}$.

The absence of decreasing $\delta^{13}\text{C}$ values in *L. fecundum* also indicates that there has been no release of methane hydrates associated with decreasing subsea permafrost recorded by the $\delta^{13}\text{C}_{\text{alga}}$ composition (Rachold et al., 2007). The large amount of ancient organic matter contained in permafrost might be involved in current biogeochemical cycling due to thawing of the upper permafrost and restoration of the

activity of viable methanogens preserved inside the permafrost (see Shakhova and Semiletov, 2007, and reference therein). However, the isotopic signatures of organic matter incorporating methane-derived carbon range from -60‰ to -65‰ (Dickens et al., 1995; Kvenvolden, 1993) relative to that of other oceanic and atmospheric carbon reservoirs with a $\delta^{13}\text{C} = 0\text{‰} \pm 7\text{‰}$ (Paull et al., 2002). Thus, if gas hydrate dissociation is observed on the East Siberian Arctic shelf (Heimann, 2010; Shakhova et al., 2010), no isotopic trace of such a phenomenon is recorded in the corallines of the Beaufort Sea Arctic shelf.

Finally, riverine influx from the Sag River can influence the surface water $\delta^{13}\text{C}_{\text{DIC}}$ and might be recorded by the $\delta^{13}\text{C}_{\text{alga}}$. As river

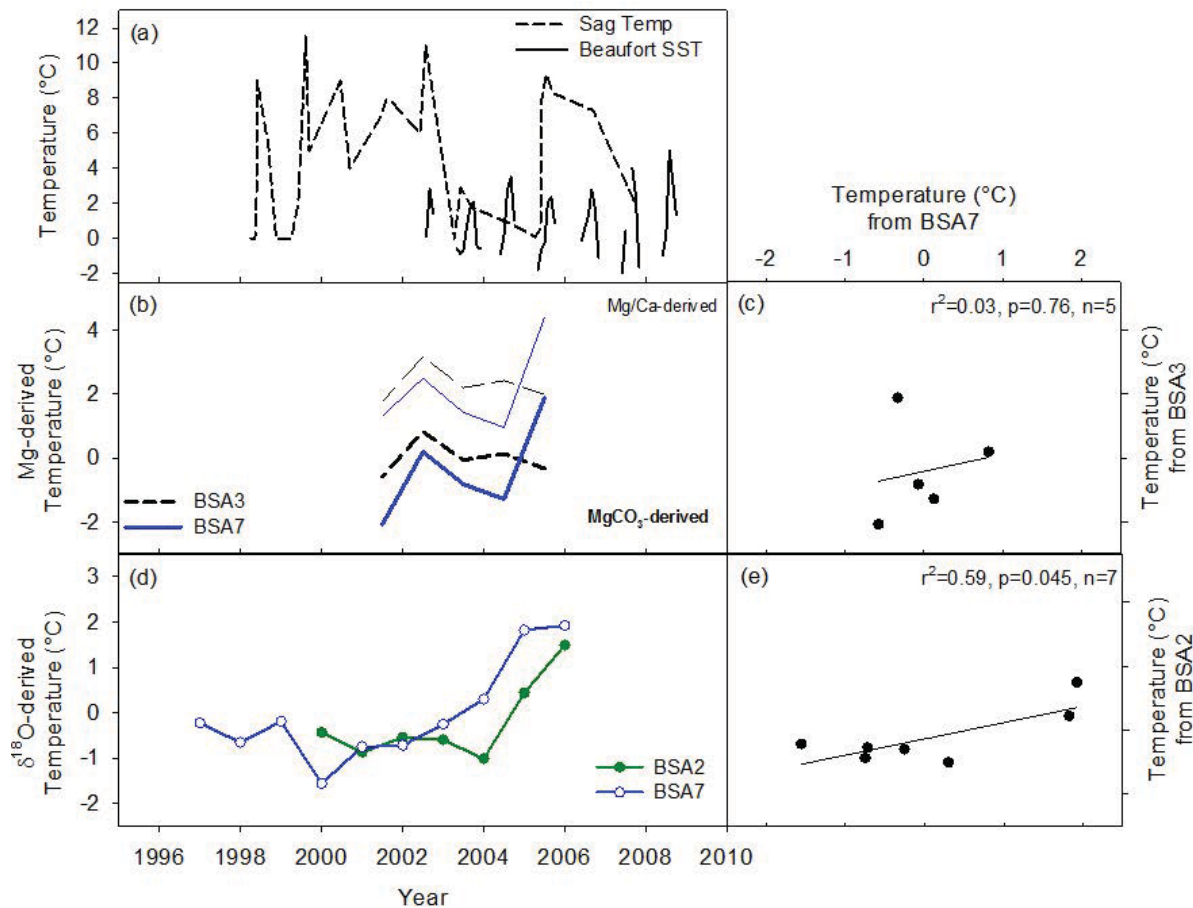


FIGURE 7. (a) Beaufort Sea (from Acker and Leptoukh, 2007) and Sagavanirktok River (from Mathew Schellekens [USGS]) water temperature; (b) seawater temperature reconstructed from *Clathromorphum nereostratum* Mg/Ca-SST relationship (top) and *Lithothamnion glaciale* MgCO₃-SST relationship (bottom); (c) BSA3 versus BSA7 seawater temperature reconstructed from the MgCO₃-SST relationship; (d) seawater temperature reconstructed from $\delta^{18}\text{O}$ composition; (e) BSA2 versus BSA7 seawater temperature reconstructed from the $\delta^{18}\text{O}$ composition.

waters tend to have a more negative carbon isotope signature than the ocean (Degens et al., 1991), we expect an anticorrelation with gage height or discharge in the $\delta^{13}\text{C}_{\text{alga}}$ recorded. However, no correlation between the variations of the river's regime and $\delta^{13}\text{C}_{\text{alga}}$ was noticed. The most likely explanation is that the proximity of the Sag River delta and sediment input in the study area disturb the record of the Beaufort Sea isotopic composition, although no clear external cause for the observed carbon isotopic record can be identified here.

Conclusion and Prospects

Leptophytum fæcundum forms a banded skeleton with large conceptacles relative to annual growth rates in the high Arctic, making image-based chronologies difficult to establish. In addition, potential growth discontinuities present in the skeleton limited the duration of paleoenvironmental records that could be extracted from the skeleton. A secondary method of dating, such as radiometric dating, is needed to verify algal age prior to the potential growth discontinuities but is difficult to do considering the young ages of the specimens. This, combined with the restricted development of the perithallium (Adey et al., 2001), limits the duration of records that are feasible to extract from *L. fæcundum*.

The absence of significant correlation between *L. fæcundum* skeletal geochemistry and environmental records further indicate the difficulties in generating paleoenvironmental records from the alga at this location. Average Mg content was similar between the two samples but varied differently over time. In addition, Mg content-derived reconstructed seawater temperatures using transfer functions developed for other taxa of coralline algae yielded temperatures that were inconsistent with satellite data. The location of the two specimens close to the discharge of the Sag River suggests a salinity influence in addition to temperature on the Mg content in *L. fæcundum*. Alternatively the algal-Mg to SST transfer functions developed for other taxa are not applicable to *L. fæcundum* or the satellite data do not accurately capture bottom temperatures that bath the coralline algae. Significant correlation of the $\delta^{18}\text{O}_{\text{alga}}$ between the two specimens supports an external environmental driver of algal skeletal $\delta^{18}\text{O}$. This driver is likely a complex combination of Beaufort Sea seawater $\delta^{18}\text{O}$ composition and temperature combined with Sag River freshwater $\delta^{18}\text{O}$ composition and temperature during high flow periods. Average $\delta^{13}\text{C}$ composition differed between the two specimens and over time. Documented changes in the source carbon to the region (e.g., $\delta^{13}\text{C}$ -Suess effect) would cause a decline in skeletal $\delta^{13}\text{C}$ values not present in the skeleton. As a result of this study, specimens of *L. fæcundum* do not appear

to provide a reliable new paleoenvironmental proxy for the Arctic Ocean, although studies of *L. foecundum* specimens removed from a freshwater influence might prove more useful.

Acknowledgments

Mathew Schellekens provided the data for Sag River. Hong Li assisted with the isotope analyses at the Geology Department at University of Toronto. Sophie Padié and Phoebe Chan provided assistance with data interpretation and statistical analyses. Analyses and visualizations of Beaufort Sea SST used in this paper were produced with the Giovanni online data system, developed and maintained by the U.S. National Aeronautics and Space Administration (NASA) Goddard Earth Sciences Data and Information Services Center (GES DISC). Funding was provided by a Natural Science and Engineering Research Council (Canada) Discovery Grant to Halfar.

References Cited

- ACIA, 2005: *Arctic Climate Impact Assessment-Scientific Report*. Cambridge University Press.
- Acker, J., and Leptoukh, G., 2007: Online analysis enhances use of NASA earth science data. *Eos, (Transactions American Geophysical Union)*, 88: 14 and 17.
- Adey, W. H., 1966: The genera *Lithothamnium*, *Leptophytum* (nov. gen.) and *Phymatolithon* in the Gulf of Maine. *Hydrobiologia*, 28: 321–370.
- Adey, W., 1965: The genus *Clathromorphum* in the Gulf of Maine. *Hydrobiologia*, 26(3/4): 539–573.
- Adey, W., 1970: The effects of light and temperature on growth rates in boreal-subarctic crustose corallines. *Journal of Phycology*, 6: 269–276.
- Adey, W., and McKibben, D., 1970: Studies on the maerl species *Phymatolithon calcareum* (Pallas) nov. comb. and *Lithothamnium coralloides* Crouan in the Ria de Vigo. *Botanica Marina*, 13: 100–106.
- Adey, W., Athanasiadis, A., and Lebednik, P., 2001: Re-instatement of *Leptophytum* and its type *Leptophytum laeve*: taxonomy and biogeography of the genera *Leptophytum* and *Phymatolithon* (Corallinales, Rhodophyta). *European Journal of Phycology*, 36: 191–203.
- Adey, W., Halfar, J., and Williams, B., 2013: Biological, physiological and ecological factors controlling high magnesium carbonate formation and producing a precision Arctic/subarctic marine climate archive: the coralline genus *Clathromorphum* Foslie emend Adey. *Smithsonian Contributions to the Marine Sciences* 40: 1–48.
- Alkire, M., and Trefry, J., 2006: Transport of spring floodwater from rivers under ice to the Alaskan Beaufort Sea. *Journal of Geophysical Research*, 111: C12008, doi <http://dx.doi.org/10.1029/2005JC003446>.
- Anderson, T., and Arthur, M., 1983: Stable isotopes of oxygen and carbon and their application to sedimentologic and paleoenvironmental problems. In Arthur, M. (ed.), *Stable Isotopes in Sedimentary Geology*. Dallas: Society for Sedimentary Geology (SEPM), pp. 1–151.
- Arrigo, K. R., Pabi, S., van Dijken, G. L., and Maslowski, W., 2010: Air-sea flux of CO₂ in the Arctic Ocean, 1998–2003. *Journal of Geophysical Research: Biogeosciences (2005–2012)*, 115(G4): doi <http://dx.doi.org/10.1029/2009JG001224>.
- Athanasiadis, A., and Adey, W. H., 2006: The genus *Leptophytum* (Melobesioideae, Corallinales, Rhodophyta) on the Pacific coast of North America. *Phycologia*, 45(1): 71–115.
- Bauch, D., Carstens, J., Wefer, G., and Thiede, J., 2000: The imprint of anthropogenic CO₂ in the Arctic Ocean: evidence from planktic δ¹³C data from watercolumn and sediment surfaces. *Deep Sea Research Part II: Topical Studies in Oceanography*, 47: 1791–1808.
- Bedard, P., Hillaire-Marcel, C., and Page, P., 1981: δ¹⁸O modelling of freshwater inputs in Baffin Bay and Canadian Arctic coastal waters. *Nature*, 293: 287–289.
- Benke, A. C., and Cushing, C. E., 2011: *Rivers of North America*. Waltham, Massachusetts: Academic Press.
- Butler, P. G., Wanamaker, A.D., Jr., Scourse, J. D., Richardson, C. A., and Reynolds, D. J., 2011: Long-term stability of δ¹³C with respect to biological age in the aragonite shell of mature specimens of the bivalve mollusk *Arctica islandica*. *Palaeogeography, Palaeoclimatology, Palaeoecology*, 302: 21–30.
- Chan, P., Halfar, J., Williams, B., Hetzinger, S., Steneck, R., Zack, T., and Jacob, D., 2011: Freshening of the Alaska Coastal Current recorded by coralline algal Ba/Ca ratios. *Journal of Geophysical Research*, 116: G01032, doi <http://dx.doi.org/10.1029/2010JG001548>.
- Chave, K., 1954. Aspects of the biogeochemistry of magnesium 1. Calcareous marine organisms. *The Journal of Geology*, 62, 266–283.
- Chave, K. and Wheeler Jr, B., 1965. Mineralogic changes during growth in the red alga, *Clathromorphum compactum*, *Science*, 147, 621, 1965.
- Cooper, L. W., Benner, R., McClelland, J. W., Peterson, B. J., Holmes, R. M., Raymond, P. A., Hansell, D. A., Grebmeier, J. M., and Codispoti, L. A., 2005: Linkages among runoff, dissolved organic carbon, and the stable oxygen isotope composition of seawater and other water mass indicators in the Arctic Ocean. *Journal of Geophysical Research: Biogeosciences (2005–2012)*, 110: doi <http://dx.doi.org/10.1029/2005JG000031>.
- Dahlgren, T. G., Weinberg, J. R., and Halanych, K. M., 2000: Phylogeography of the ocean quahog (*Arctica islandica*): influences of paleoclimate on genetic diversity and species range. *Marine Biology*, 137: 487–495.
- Degens, E. T., Kempe, S., and Richey, J. E., 1991: SCOPE 42: Biogeochemistry of Major World Rivers. Chichester, U.K.: Wiley.
- Dickens, G. R., O’Neil, J. R., Rea, D. K., and Owen, R. M., 1995: Dissociation of oceanic methane hydrate as a cause of the carbon isotope excursion at the end of the Paleocene. *Paleoceanography*, 10: 965–971.
- Dickson, R., Rudels, B., Dye, S., Karcher, M., Meincke, J., and Yashayaev, I., 2007: Current estimates of freshwater flux through Arctic and subarctic seas. *Progress in Oceanography*, 72: 210–230.
- Ferguson, J., Henderson, G., Kucera, M., and Rickaby, R., 2008: Systematic change of foraminiferal Mg/Ca ratios across a strong salinity gradient. *Earth and Planetary Science Letters*, 265: 153–166.
- Grottoli, A., and Eakin, C., 2007: A review of modern coral δ¹⁸O and Δ¹⁴C proxy records. *Earth Science Reviews*, 81: 67–91.
- Halfar, J., Zack, T., Kronz, A., and Zachos, J., 2000: Growth and high-resolution paleoenvironmental signals of rhodoliths (coralline red algae): a new biogenic archive. *Journal of Geophysical Research*, 105: 22107–22116, doi <http://dx.doi.org/10.1029/1999JC000128>.
- Halfar, J., Steneck, R., Joachimski, M., Kronz, A., and Wanamaker, A., Jr., 2008: Coralline red algae as high-resolution climate recorders. *Geology*, 36: 463–466, doi <http://dx.doi.org/10.1130/G24635A.24631>.
- Halfar, J., Adey, W., Kronz, A., Hetzinger, S., Edinger, E., and Fitzhugh, W., 2013: Arctic sea-ice decline archived by multicentury annual-resolution record from crustose coralline algal proxy. *Proceedings of the National Academy of Sciences*, 110(49): 19737–19741, doi <http://dx.doi.org/10.1073/pnas.1313775110>.
- Heimann, M., 2010: How stable is the methane cycle? *Science* 327: 1211–1212.
- Hetzinger, S., Halfar, J., Kronz, A., Steneck, R., Adey, W., Lebednik, P., and Schöne, B., 2009: High-resolution Mg/Ca ratios in a coralline red alga as a proxy for Bering Sea temperature variations from 1902 to 1967. *Palaeos*, 24: 406–412, doi <http://dx.doi.org/10.2110/palo.2008.p2108-2116r>.
- Hetzinger, S., Halfar, J., Zack, T., Mecking, J., Kunz, B., Jacob, D., and Adey, W., 2013: Coralline algal barium as indicator for 20th century northwestern North Atlantic surface ocean freshwater variability. *Scientific Reports*, 3: 1761, doi <http://dx.doi.org/10.1038/srep01761>.
- Jahn, A., and Holland, M., 2013: Implications of Arctic sea ice changes for North Atlantic deep convection and the meridional overturning circulation in CCSM4-CMIP5 simulations. *Geophysical Research Letters*, 40: 1206–1211, doi <http://dx.doi.org/10.1029/2012GL05183>.

- Jiménez-López, C., Romanek, C., Huertas, F., Ohmoto, H., and Caballero, E., 2004: Oxygen isotope fractionation in synthetic magnesian calcite. *Geochimica et Cosmochimica Acta*, 68: 3367–3377, doi <http://dx.doi.org/3310.1016/j.gca.2003.3311.3033>.
- Kamenos, N., 2011: North Atlantic summers have warmed more than winters since 1353, and the response of marine zooplankton. *Proceedings of the National Academy of Sciences*, 107: 22442–22447, doi <http://dx.doi.org/22410.21073/pnas.1006141107>.
- Kamenos, N., Cusack, M., and Moore, P., 2008: Coralline algae are global paleothermometers with bi-weekly resolution. *Geochimica et Cosmochimica Acta*, 72: 771–779, doi <http://dx.doi.org/710.1016/j.gca.2007.1011.1019>.
- Kamenos, N., Hoey, T., Nienow, P., Fallick, A., and Claverie, T., 2012: Reconstructing Greenland ice sheet runoff using coralline algae. *Geology*, 40: 1095–1098, doi <http://dx.doi.org/1010.1130/G33405.33401>.
- Kaufman, D. S., Schneider, D. P., McKay, N. P., Ammann, C. M., Bradley, R. S., Briffa, K. R., Miller, G. H., Otto-Bliesner, B. L., Overpeck, J. T., and Vinther, B. M., 2009: Recent warming reverses long-term Arctic cooling. *Science*, 325: 1236–1239.
- Kennett, J. P., Cannariato, K., Hendy, I., and Behl, R., 2003: Methane hydrates in Quaternary climate change: the clathrate gun hypothesis. Washington, D.C.: American Geophysical Union.
- Kerr, R., 2010: “Arctic Armageddon” needs more science, less hype. *Science*, 329: 620–621.
- Kısakürek, B., Eisenhauer, A., Böhm, F., Garbe-Schönberg, D., and Erez, J., 2008: Controls on shell Mg/Ca and Sr/Ca in cultured planktonic foraminiferan, *Globigerinoides ruber* (white). *Earth and Planetary Science Letters*, 273: 260–269.
- Kline, T., Wilson, W., and Goering, J., 1998: Natural isotope indicators of fish migration at Prudhoe Bay, Alaska. *Canadian Journal of Fisheries and Aquatic Sciences*, 55: 1494–1502.
- Kolesar, P. Magnesium in calcite from a coralline alga, 1978. *Journal of Sedimentary Petrology* 48, 815–820.
- Kvenvolden, K. A., 1993: Gas hydrates—geological perspective and global change. *Reviews of Geophysics*, 31: 173–187.
- Lear, C. H., Rosenthal, Y. & Slowey, N., 2002. Benthic foraminiferal Mg/Ca-paleothermometry: A revised core-top calibration. *Geochimica et Cosmochimica Acta* 66, 3375–3387.
- Lorrain, A., Paulet, Y.-M., Chauvaud, L., Dunbar, R., Mucciarone, D., and Fontugne, M., 2004: $\delta^{13}\text{C}$ variation in scallop shells: increasing metabolic carbon contribution with body size? *Geochimica et Cosmochimica Acta*, 68: 3509–3519.
- Moberly, R., 1968: Composition of magnesian calcites of algae and pelecypods by electron microprobe analysis. *Sedimentology*, 11: 61–82.
- Nozaki, Y., Rye, D., Turekian, K., and Dodge, R., 1978: A 200 year record of carbon 13 and carbon 14 variations in a Bermuda coral. *Geophysical Research Letters*, 5: 825–828.
- Overpeck, J., Hughen, K., Hardy, D., Bradley, R., Case, R., Douglas, M., Finney, B., Gajewski, K., Jacoby, G., Jennings, A., Lamoureux, S., Lasca, A., MacDonald, G., Moore, J., Retelle, M., Smith, S., Wolfe, A., and Zielinski, G., 1997: Arctic environmental change of the last four centuries. *Science*, 278: 1251–1256.
- Pabi, S., van Dijken, G., and Arrigo, K., 2008: Primary production in the Arctic Ocean, 1998–2006. *Journal of Geophysical Research*, 113: C08005, doi <http://dx.doi.org/08010.01029/02007JC004578>.
- Paillard, D., Labeyrie, L., and Yiou, P., 1996: Macintosh program performs timeseries analysis. *Eos (Transactions, American Geophysical Union)*, 77: 379.
- Paull, C., Brewer, P., Ussler, W., Peltzer, E., Rehder, G., and Clague, D., 2002: An experiment demonstrating that marine slumping is a mechanism to transfer methane from seafloor gas-hydrate deposits into the upper ocean and atmosphere. *Geo-Marine Letters*, 22: 198–203.
- Perovich, D. K., Light, B., Eicken, H., Jones, K. F., Runciman, K., and Nghiem, S. V., 2007: Increasing solar heating of the Arctic Ocean and adjacent seas, 1979–2005: attribution and role in the ice-albedo feedback. *Geophysical Research Letters*, 34.
- Pickart, R., Schulze, L., Moore, G., Charette, M., Arrigo, K., van Dijken, G., and Danielson, S., 2013: Long-term trends of upwelling and impacts on primary productivity in the Alaskan Beaufort Sea. *Deep Sea Research Part I: Oceanographic Research Papers*, 79: 106–121.
- Rachold, V., Bolshiyarov, D. Y., Grigoriev, M. N., Hubberten, H. W., Junker, R., Kunitzky, V. V., Merker, F., Overduin, P., and Schneider, W., 2007: Nearshore Arctic subsea permafrost in transition. *Eos (Transactions American Geophysical Union)*, 88: 149–150.
- Rennermalm, A., Wood, E., Weaver, A., Eby, M., and Dery, S., 2007: Relative sensitivity of the Atlantic meridional overturning circulation to river discharge into Hudson Bay and the Arctic Ocean. *Journal of Geophysical Research: Biogeosciences (2005–2012)*, 112: doi <http://dx.doi.org/10.1029/2006JG000330>.
- Rosenheim, B., Swart, P., Thorrold, S., Willenz, P., Berry, L., and Latkoczy, C., 2004: High-resolution Sr/Ca records in sclerosponges calibrated to temperature in situ. *Geology*, 32: 145–148.
- Schmidt, G., Bigg, G., and Rohling, E., 1999: Global Seawater Oxygen-18 Database. <http://data.giss.nasa.gov/o18data>.
- Schöne, B., 2013: *Arctica islandica* (Bivalvia): a unique paleoenvironmental archive of the northern North Atlantic Ocean. *Global and Planetary Change*, 111: 199–225.
- Shakhova, N., and Semiletov, I., 2007: Methane release and coastal environment in the East Siberian Arctic shelf. *Journal of Marine Systems*, 66: 227–243.
- Shakhova, N., Semiletov, I., Salyuk, A., Yusupov, V., Kosmach, D., and Gustafsson, Ö., 2010: Extensive methane venting to the atmosphere from sediments of the East Siberian Arctic Shelf. *Science*, 327: 1246–1250.
- Steffensen, J. P., Andersen, K. K., Bigler, M., Clausen, H. B., Dahl-Jensen, D., Fischer, H., Goto-Azuma, K., Hansson, M., Johnsen, S. J., and Jouzel, J., 2008: High-resolution Greenland ice core data show abrupt climate change happens in few years. *Science*, 321: 680–684.
- Suess, H., 1953: Natural radiocarbon and the rate of exchange of carbon dioxide between the atmosphere and the sea. *Nuclear Processes in Geologic Settings*, 43: 52–56.
- Swart, P., Greer, L., Rosenheim, B., Moses, C., Waite, A., Winter, A., Dodge, R., and Helmle, K., 2010: The ^{13}C Suess effect in scleractinian corals mirror changes in the anthropogenic CO_2 inventory of the surface oceans. *Geophysical Research Letters*, 37: L05604, doi <http://dx.doi.org/05610.01029/02009GL041397>.
- Tremblay, J.-E., Belanger, S., Barber, D., Asplin, M., Martin, J., Darnis, G., Fortier, L., Gratton, Y., Link, H., Archambault, P., Sallon, A., Michel, C., Williams, W., Philippe, B., and Gosselin, M., 2011: Climate forcing multiplies biological productivity in the coastal Arctic Ocean. *Geophysical Research Letters*, 38: doi <http://dx.doi.org/10.1029/2011GL048825>.
- Urey, H., 1947: The thermodynamic properties of isotopic substances. *Journal of the Chemical Society (London)*: 562–581.
- Wanamaker, A. D., Hetzinger, S., and Halfar, J., 2011: Reconstructing mid- to high-latitude marine climate and ocean variability using bivalves, coralline algae, and marine sediment cores from the northern hemisphere. *Palaeogeography, Palaeoclimatology, Palaeoecology*, 302: 1–9.
- Williams, B., Halfar, J., Steneck, R., Wortmann, U., Hetzinger, S., Adey, W., Lebednik, P., and Joachimski, M., 2011: Twentieth century $\delta^{13}\text{C}$ variability in surface water dissolved inorganic carbon recorded by coralline algae in the northern North Pacific Ocean and the Bering Sea. *Biogeosciences*, 8: 165–174, doi <http://dx.doi.org/110.5194/bg-5198-5165-2011>.
- Williams, B., Halfar, J., DeLong, K., Hetzinger, S., Steneck, R., and Jacob, D., 2014: Multi-specimen and multi-site calibration of Aleutian coralline algal Mg/Ca to climate signals. *Geochimica et Cosmochimica Acta*, 139: 190–204.

MS accepted December 2014

APPENDIX

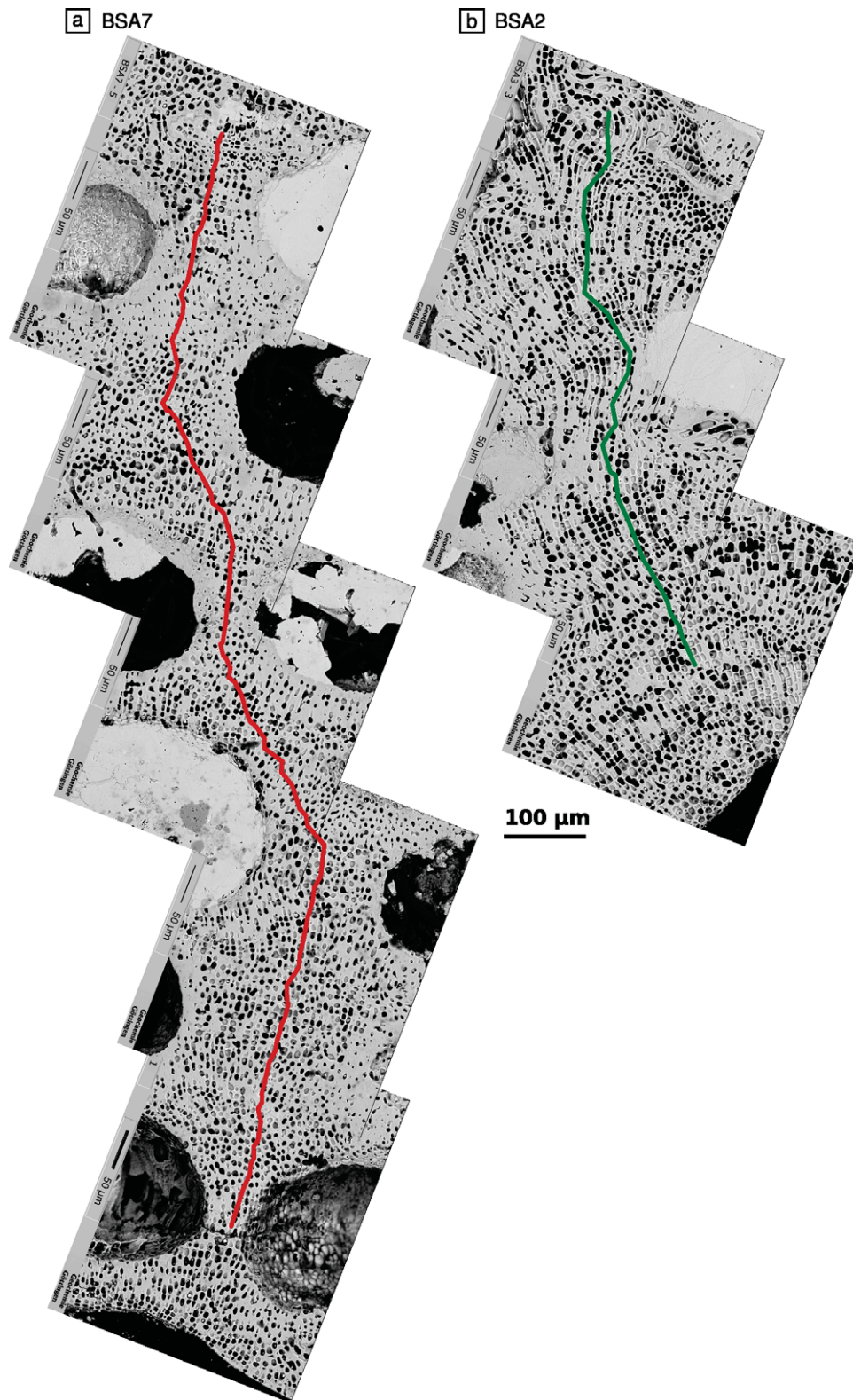


FIGURE A1. Microprobe analysis and algal chronology. Red and green lines indicate position of measurement transects.